Available online at www.sciencedirect.com

ScienceDirect

Ceramics International 40 (2014) 4203–4206

CERAMICS INTERNATIONAL

www.elsevier.com/locate/ceramint

# Preparation and characterization of single crystalline $In_2O_3$ films deposited on MgO (110) substrates by MOCVD

Zhao Li, Cansong Zhao, Wei Mi, Caina Luan, Xianjin Feng, Jin Ma*

*School of Physics, Shandong University, Jinan 250100, PR China*

Received 7 July 2013; received in revised form 7 July 2013; accepted 19 August 2013
Available online 28 August 2013

**Abstract**

Epitaxial indium oxide ($In_2O_3$) films have been prepared on MgO (110) substrates by metal-organic chemical vapor deposition (MOCVD). The deposition temperature varies from 500 °C to 700 °C. The films deposited at each temperature display a cube-on-cube orientation relation with respect to the substrate. The $In_2O_3$ film deposited at 600 °C exhibits the best crystalline quality. A clear epitaxial relationship of $In_2O_3$ (110) ∥MgO (110) with $In_2O_3$ [001]∥MgO [001] has been observed from the interface area between the film and the substrate. The average transmittance of the prepared films in the visible range is over 95%. The band gap of the obtained $In_2O_3$ films is about 3.55–3.70 eV.


*Keywords:* C. Optical properties; Indium oxide; Crystal structure; MOCVD

## 1. Introduction

In recent years, people have always focused their attentions on wide band gap transparent oxide semiconductors (TOSs) due to the huge commercial desire for transparent photoelectron devices [1,2]. $In_2O_3$, with a band gap of 3.7 eV [3], is a very important TOS material owing to its physically stability and chemically inertness. In virtue of its outstanding optical and electrical properties, $In_2O_3$ film has been widely used in many fields such as light-emitting diodes, photovoltaic devices, flat-panel displays, gas sensors [4–8] and so on. To date, various methods for the preparation of $In_2O_3$ films have been described in the literature, including magnetron sputtering [9], molecular beam epitaxy [10], electron beam evaporation [11], pulsed laser deposition (PLD) [12] and MOCVD [13,14]. The MOCVD method is appropriate for preparation of thin films because of the easy modulation of deposition rate and the large throughput fit for commercialized production.

In the former study, most of the reported $In_2O_3$ films are polycrystalline films. Only a few reports concerning the growth of single crystal $In_2O_3$ films can be found in the literature. Zhang et al. [15], reported the epitaxial growth of $In_2O_3$ thin films on the substrate of YSZ (111). In the previous work of our group, single crystalline $In_2O_3$ films have been successfully deposited on MgO (100) substrate [16]. Nevertheless, the $In_2O_3$ films deposited on MgO (100) substrate were epitaxial films with domain structure [16]. In this letter, the fabrication and properties of high-quality single crystalline $In_2O_3$ films without domain structure deposited on MgO (110) by MOCVD have been investigated.

## 2. Experiment details

The growth of $In_2O_3$ films was performed on MgO (110) substrates by using a high vacuum MOCVD system. Commercial available MgO (110) wafers (double-polished, size of 10 mm × 10 mm × 0.5 mm) are used for substrate. Trimethylindium [$In(CH_3)_3$, 6 N in purity], which is commercially available, was used as the organometallic (OM) source. The OM bubbler was maintained at a temperature of 15 °C with a pressure of 300 Torr. Its vapor was transported into the reactor with a flow rate of 9 sccm (standard-state cubic centimeter per minute) by ultrahigh-purity nitrogen (9 N in purity) as the carrier gas. So the accurate flow rate of the OM vapor was calculated as a value of $1.5 \times 10^{-6}$ mol/min. High

*Corresponding author. Tel.: +86 531 88361057.
*E-mail address:* lee929412@gmail.com (J. Ma).

0272-8842/$ - see front matter © 2013 Elsevier Ltd and Techna Group S.r.l. All rights reserved.
http://dx.doi.org/10.1016/j.ceramint.2013.08.078

purity $O_2$ (5 N) was injected as oxidant with a flow rate of 50 sccm using a separate delivery line into the reactor. During the deposition (5 h for each sample), the growth pressure was kept at 20 Torr and the substrate temperature ($T_s$) was set at a certain value ranging from 500 °C to 700 °C.

The microstructure and the epitaxial relationship of the deposited samples were examined by X-ray diffraction (XRD) and high-resolution transmission electron microscopy (HRTEM). The $\theta$–$2\theta$ scans of XRD were performed by using a Bruker D8 Advance X-ray diffractometer with Cu Kα1 radiation. In-plane $\Phi$-scans were performed by using a Bede D1 HR-XRD. When it comes to the HRTEM measurement, the samples should be treated specially. Samples in cross-sections orientation were prepared by gluing two pieces together with $In_2O_3$ films facing each other, followed by grinding and mechanical polishing, and finally by ion-beam thinning ($Ar^+$, 4.5 kV) at incidence angles of 10–6°.This process is to get a very thin area which is electron transparent. Selected area electron diffraction (SAED) and HRTEM were then performed on the sample using a Tecnai F30 transmission electron microscope operated at 300 kV. To measure the optical transmittance spectra in the wavelength range of 200–800 nm, a homemade TU-1901 double-beam UV–vis–NIR spectrophotometer was used.

## 3. Results and discussion

Typical $\theta$–$2\theta$ scans of XRD spectra for $In_2O_3$ films grown at different $T_s$ are displayed in Fig. 1. It can be seen that, in addition to the peak corresponding to substrate MgO (220), only one strong peak corresponding to $In_2O_3$ (440) reflection is observed regardless of the $T_s$. The result indicates that the deposited samples are pure $In_2O_3$ films of body centered cubic (bcc) structure with a single out-of-plane orientation of $In_2O_3$ (110)∥MgO(110). When the $T_s$ increases from 500 °C to 700 °C, the location of the $In_2O_3$ (440) peak does not change evidently. The full width at half maximum (FWHM) of $In_2O_3$ (440) peak is 0.34, 0.32, 0.27, 0.35 and 0.34 corresponding to $T_s$ of 500, 550, 600, 650 and 700 °C, respectively. These observations imply that the $T_s$ significantly affects the structure of the films and the sample deposited at 600 °C exhibits the best crystalline quality.

Fig. 2(a) and (b) displays the XRD off-specular $\Phi$-scans of the (400) reflection ($\psi$=45°) for the $In_2O_3$ (440) film and the (200) reflection ($\psi$=45°) for the MgO (220) substrate at a fixed position. It should be noted that the tilt angle ($\psi$) is the angle between the reflection plane and substrate surface plane. In Fig. 2(b), two peaks separated by 180° are measured. As we know, the MgO (200) plane is two-fold symmetrical along the MgO [110] direction, corresponding to the two peaks in curve (b). Fig. 2(a) is almost the same with Fig. 2(b), which also means the existence of two-fold symmetrical structure and there is no domain structure inside the $In_2O_3$ film.

In order to explain the structure relationship between the film and the substrate, a proposed schematic diagram of growth mechanism has been schematically shown in Fig. 3 (a) and (b), which are the geometrical configurations of the MgO (110) and $In_2O_3$ (110) surfaces from the plan-view observation. The MgO substrate we used has a cubic structure

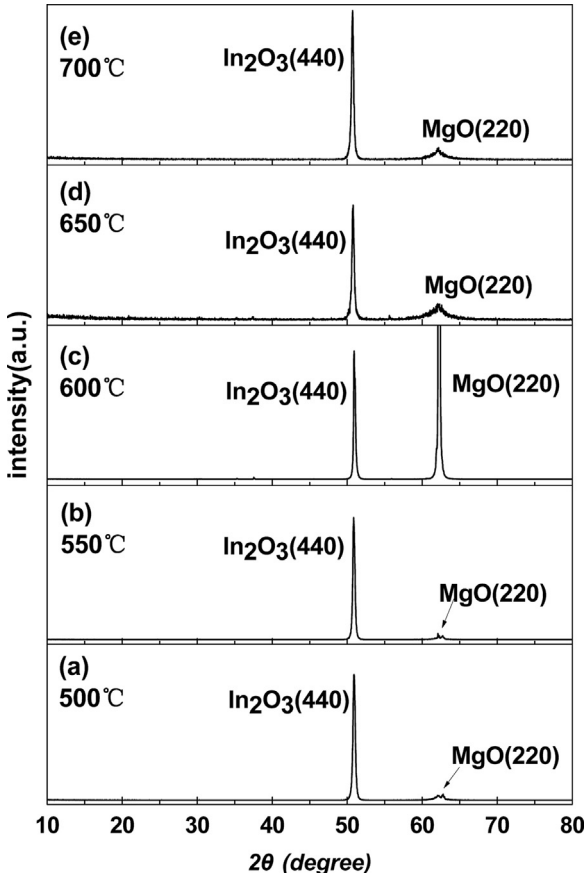


Fig. 1. XRD spectra of the $In_2O_3$ films prepared on MgO (110) at different $T_s$.

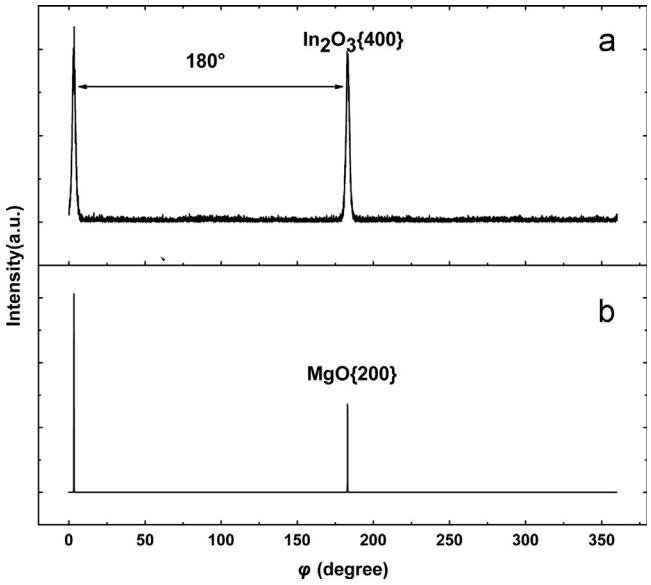


Fig. 2. XRD off-specular $\Phi$-scans of (a) $In_2O_3$ {400} and (b) MgO {200} planes for the sample at a fixed position.

with a lattice parameter of $a$=4.211 Å, and the lattice parameter of bcc $In_2O_3$ is $a'$=10.118 Å (JCPDS 06-0416). From Fig. 3(a) and (b), the lattice mismatch between the 28.618 Å ($In_2O_3$ [$\bar{1}$10] orientation) and 29.775 Å (MgO [$\bar{1}$10] orientation) is 3.9%, the 20.236 Å ($In_2O_3$ [001] orientation)

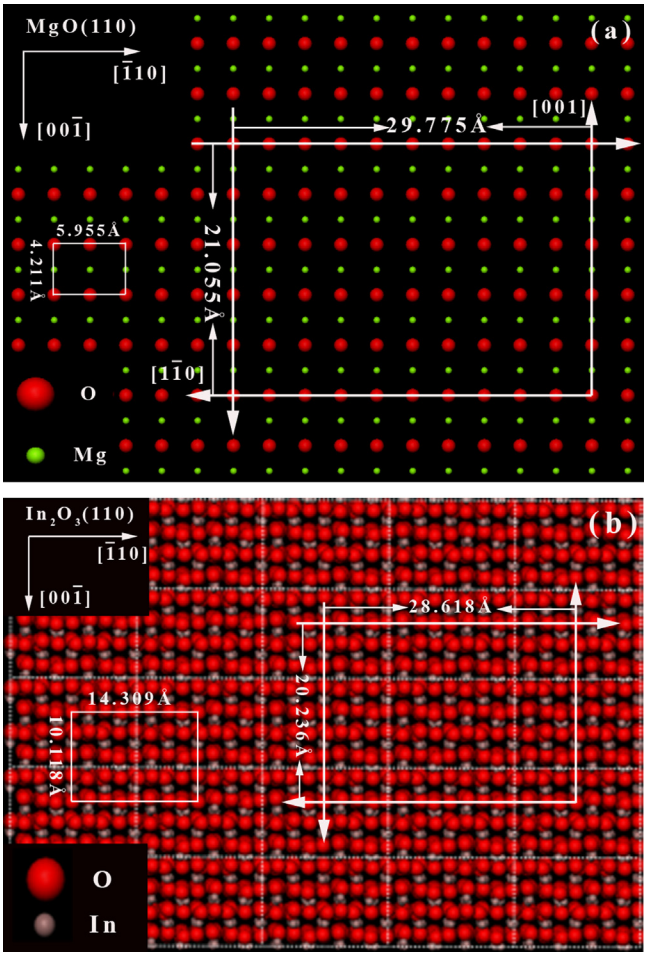


Fig. 3. (a) and (b) are the schematic diagrams of geometrical epitaxial relationship between $In_2O_3$ film and MgO substrate.

and 21.055 Å (MgO [001] orientation) is also 3.9%. So the in-plane epitaxial relationship can be given as [001] $In_2O_3$ ∥ [001] MgO and [1̄10] $In_2O_3$ ∥ [1̄10] MgO.

The low magnification cross-sectional transmission electron microscopy (XTEM) image of the $In_2O_3$ sample prepared at the temperature of 600 °C is illustrated in Fig. 4(a). Fig. 4(b) shows the HRTEM image of the interface area between the $In_2O_3$ film and MgO substrate, while Fig. 4(c) is the corresponding SAED pattern. From image (a), the thickness of the film is about 395 nm, and a clear interface between the $In_2O_3$ film and the MgO substrate is observed. For the HRTEM image, the incident electron beam is parallel to the (001) direction of the MgO substrate. The interface and the lattice of the sample can be seen clearly. It is shown that the deposited film is structurally uniform single crystalline and the growth direction of $In_2O_3$ film is [440]. For the substrate, the interface spacings marked by the arrows are 0.143 and 0.212 nm, which are consistent with MgO (220) and (200), respectively. For the film, the interplane spacings are 0.176 nm and 0.225 nm, corresponding to $In_2O_3$ (440) and (400). The SAED pattern clearly shows the diffraction spots of $In_2O_3$ (440), (200), (420) planes obviously, in which the diffraction spots of MgO (220) and (200) planes are also clearly observed. The HRTEM and SAED analyses of the interface for the sample show a cube-on-cube epitaxial relationship of $In_2O_3$ (110) ∥ MgO (110) with $In_2O_3$ [001] ∥ MgO [001], which is consistent with the XRD analyses.

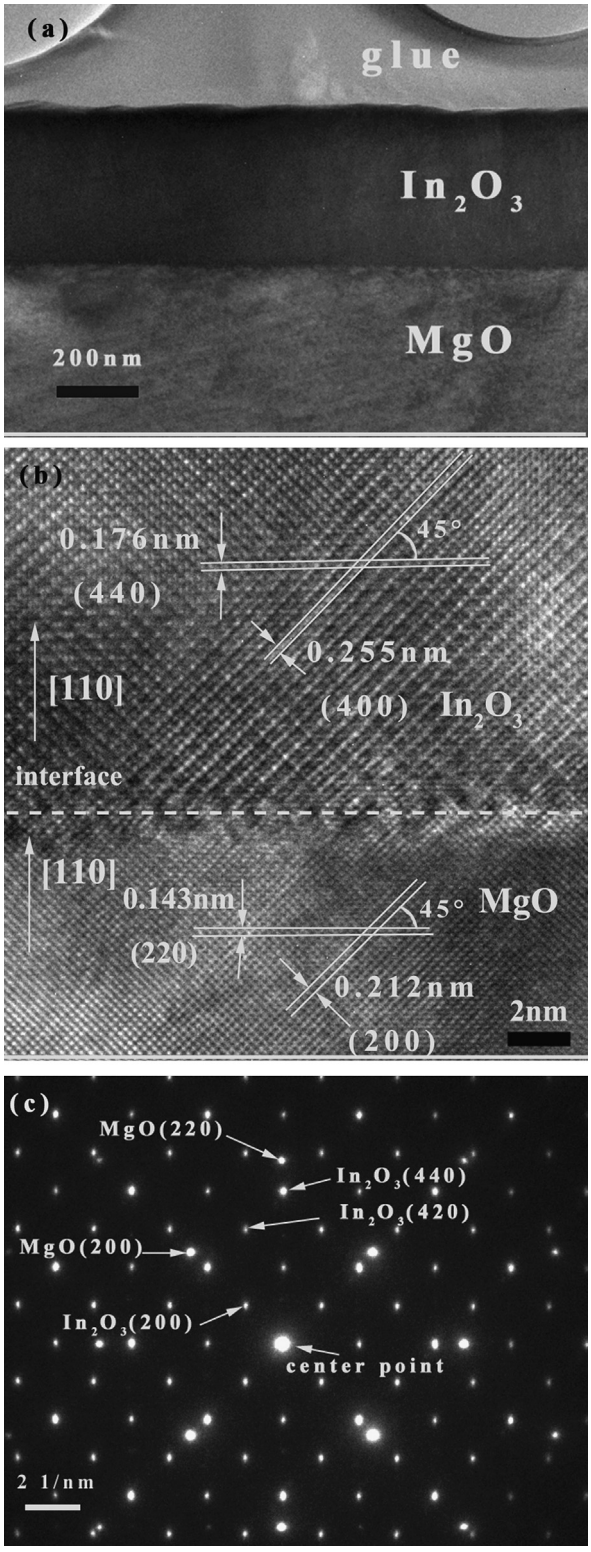


Fig. 4. The cross-section (a) low magnification XTEM image, (b) HRTEM image, and (c) SAED micrographs of the interface area between the $In_2O_3$ film and the MgO substrate.

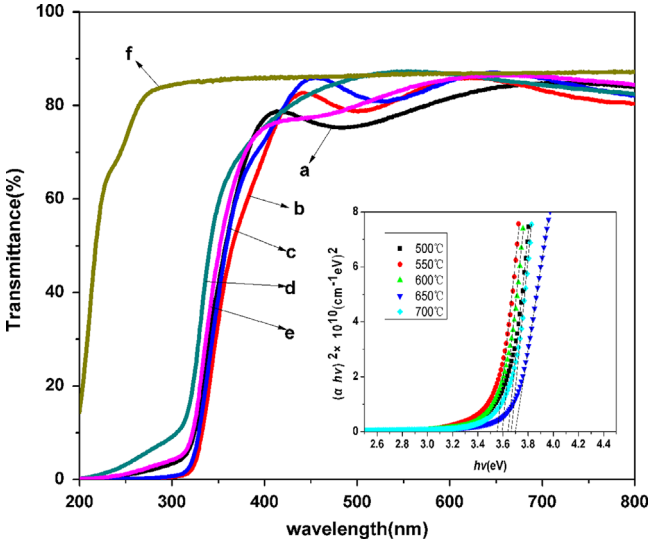


Fig. 5. Optical transmittance spectra of the $In_2O_3$ samples and the MgO substrate, with the plot of $(\alpha h\upsilon)^2$ vs. $h\upsilon$ in the inset.

The transmittance spectra as a function of wavelength in the range of 200–800 nm is shown in Fig. 5. Curves a–f correspond to the samples deposited at different $T_s$ of 500–700 °C and the MgO substrate. The average transmittance of each sample in the visible range is over 80%, and the absolute average transmittance of each sample exceeds 95% deducting the influence of the substrate (of 85% for MgO). For direct transition semiconductors, the absorption coefficient ($\alpha$) and optical band gap ($E_g$) are related by [17]

$$\alpha h\upsilon = A(h\upsilon - E_g)^{1/2} \quad (1)$$

where $h\upsilon$ is the energy of the incident photon and $A$ is a material dependent constant. The plot of $(\alpha h\upsilon)^2$ as a function of $h\upsilon$ is shown in the inset of Fig. 5, in which the intercept of the tangent to the plot gives a good approximation of the optical band gap. By this way of calculation, the optical band gap ($E_g$) is estimated to be 3.64, 3.55, 3.59, 3.70 and 3.66 eV corresponding to the films deposited at $T_s$ of 500, 550, 600, 650 and 700 °C, respectively. These results show that the obtained $In_2O_3$ films have excellent transparency in the visible wavelength region and is sure to be widely used in the field of optoelectronic devices.

## 4. Conclusion

Epitaxial $In_2O_3$ films with bcc structure have been deposited on MgO (110) substrates at different growth temperatures by MOCVD. The XRD analyses show that the film deposited at 600 °C exhibits the best crystallinity. A schematic diagram is proposed to clarify the growth mechanism, which shows the epitaxial relationship of $In_2O_3$ (110)∥MgO (110) with $In_2O_3$ [001]∥MgO [001]. The absolute average transmittance of the samples in visible range is over 95%, and the optical band gap of the obtained films is about 3.55–3.70 eV. High optical transmittance within visible region is a key point of transparent oxide materials for the wide application in optoelectronic devices.

## Acknowledgments

This work is supported by the National Natural Science Foundation of China (Grant no. 51272138) and the Independent Innovation Foundation of Shandong University (Grant no. 2013TB007).

## References

[1] J.F. Wager, Transparent electronics, Science 300 (2003) 1245.
[2] B.G. Lewis, D.C. Paine, Applications and processing of transparent conducting oxides, Materials Research Society Bulletin 25 (2000) 22.
[3] S. Mirzapour, S.M. Rozati, M.G. Takwale, B.R. Marathe, V.G. Bhide, Dependence of structural and electrical properties of undoped spray-deposited indium oxide thin films on deposition temperature, Materials Letters 13 (1992) 275.
[4] J. Lao, J. Huang, D. Wang, Z.F. Ren, Self-assembled $In_2O_3$ nanocrystal chains and nanowire networks, Advanced Materials 16 (2004) 65.
[5] C.G. Granqvist, Transparent conductive electrodes for electrochromic devices: a review, Applied Physics A 57 (1993) 19.
[6] Y. Zhang, H. Ago, J. Liu, M. Yumura, K. Uchida, S. Ohshima, S. Iijima, J. Zhu, X. Zhang, The synthesis of In, $In_2O_3$ nanowires and $In_2O_3$ nanoparticles with shape-controlled, Journal of Crystal Growth 264 (2004) 363.
[7] H. Hosono, Recent progress in transparent oxide semiconductors: materials and device application, Thin Solid Films 515 (2007) 6000.
[8] A. Tsukazaki, A. Ohtomo, T. Kita, Y. Ohno, H. Ohno, M. Kawasaki, Quantum hall effect in polar oxide heterostructures, Science 315 (2007) 1388.
[9] S. Kasiviswanathan, G. Rangarajan, Direct current magnetron sputtered $In_2O_3$ films as tunnel barriers, Journal of Applied Physics 75 (1994) 2572.
[10] N. Taga, M. Maekwa, Y. Shigesato, I. Yasui, M. Kakei, T.E. Haynes, Deposition of heteroepitaxial $In_2O_3$ thin films by molecular beam epitaxy, Japanese Journal of Applied Physics 37 (1998) 6524.
[11] T. Maruyama, K. Fukui, Indium-tin oxide thin films prepared by chemical vapor deposition, Journal of Applied Physics 70 (1991) 3848.
[12] H. Ohta, M. Orita, M. Hirano, H. Hosono, Surface morphology and crystal quality of low resistive indium tin oxide grown on yittria-stabilized zirconia, Journal of Applied Physics 91 (2002) 3547.
[13] Lingyi Kong, Jin Ma, Fan Yang, Zhen Zhu, Caina Luan, Hongdi Xiao, Characterization of single-crystalline $In_2O_3$ films deposited on Y-stabilized $ZrO_2$ (100) substrates by MOCVD, Applied Surface Science 257 (2010) 518.
[14] Ch.Y. Wang, V. Lebedev, V. Cimdalla, Th. Kups, K. Tonisch, O. Ambacher, Structural studies of single crystalline $In_2O_3$ films epitaxially grown on InN (0001), Applied Physics Letters 90 (2007) 221902.
[15] K.H.L. Zhang, V.K. Lazarov, H.H.-C. Lai, R.G. Egdell, Influence of temperature on the epitaxial growth of $in_2o_3$ thin films on Y-$ZrO_2$ (111), Journal of Crystal Growth 318 (2011) 345.
[16] Lingyi Kong, Jin Ma, Caina Luan, Zhen Zhu, Qiaoqun Yu, Domain Structure and optical property of epitaxial indium oxide film deposited on MgO (100) substrate, Surface Science 605 (2011) 977.
[17] D. Beena, K.J. Lethy, R. Vinodkumar, V.P.M. Pillai, V. Ganesan, D. M. Phase, S.K. Sudheer, Effect of Substrate temperature on structural, optical and electrical properties of pulsed laser ablated nanostructured indium oxide films, Applied Surface Science 255 (2009) 8334.